CHAPTER 6

FEASIBILITY STUDY OF EXISTING POWER PLANT SHELL AND TUBE CONDENSER USING HYBRID NANOFLUIDS

In this chapter, the energy, exergy and economic assessments of existing shell and tube type condenser are investigated numerically by using various hybrid nanofluids (Al_2O_3+MWCNT/water, Al_2O_3+Ag/water, Al_2O_3+Cu/water, Al_2O_3+TiO_2/water and Al_2O_3+PCM/water) as a coolant. Effects of nanoparticle and PCM volume concentration on overall heat transfer coefficient, coolant flow rate, pumping power, irreversibility, exergetic efficiency and annual cost are investigated. Also, the payback period is determined to measure the duration in which the use of hybrid nanofluids would be profitable.

6.1 Modeling and Simulation

An industrial condenser of steam power plant (Nuclear Power Corporation of India Limited, Tarapur) has been considered in the present study for performance assessment using different hybrid nanofluids. Five different types of water-based hybrid nanofluids (Al_2O_3+MWCNT, Al_2O_3+Ag, Al_2O_3+Cu, Al_2O_3+TiO_2 and Al_2O_3+PCM with 50/50 ratio) at overall volume concentration ranging (0-1%) have been taken for investigation. This range of volume concentration has been taken for two purposes, (i) the cost of the nanoparticles reduces as low concentration means low cost of nanoparticles and (ii) to avoid the instability of the nanofluids. The instability of nanofluid can inhibit its performance in several applications such as heat exchanger, chemical industry application, enhanced oil recovery, etc. The instability of nanofluids is caused due to the propensity of nanoparticles to form a cluster in the fluid. Higher concentration means low stability of the nanofluids. Capric acid has used as PCM because of its melting point, which is in the considered temperature range

to take advantage of phase change. **Table 6.1** shows the thermophysical properties of different nanoparticles and base fluid. The general layout of the condenser cooling system is shown in Fig 6.1. The exhausted steam from the low-pressure turbine passes through the shell side of the condenser with a flow rate of 270.645 kg/s and the coolant passes through the tube side. The temperature of the condensate at the hot well outlet was maintained at 42.6^{o}C. The inlet temperature of the coolant was taken the same as that of the ambient temperature, i.e., 29^{o}C. The specification of shell and tube condenser and operating conditions data of steam were taken from the power plant station, as shown in Table 6.2. The simulation model has been executed using EES (Engineering Equation Solver). The following assumptions have been made for simulation:

- The condenser is assigned to convert steam (quality of steam, x=0.9) into saturated water (x=0); neither superheating nor subcooling is considered.
- Heat transfer occurs in condenser among steam and coolant only; no heat interaction with surroundings.
- The efficiency of the coolant pump has been taken as 85%.
- Ambient temperature has been taken as the inlet temperature of the coolant, i.e., 29^{o}C.

Table 6.1. Thermophysical properties of base fluid and nanoparticles.

Materials	**Shape**	**Thermal conductivity (W/m. K)**	**Density (Kg/m^3)**	**Specific heat (J/kg. K)**	**Viscosity (Pa. s)**	**Latent heat (kJ/kg)**
Water	------	0.606	995	4183	0.0007623	-------
Al_2O_3	Spherical	40	3900	880	-------	-------
MWCNT	Cylindrical	3000	2600	740	-------	-------
TiO_2	Spherical	11.7	4260	697	-------	--------
Ag	Spherical	425	10500	235	--------	-------

Cu	Spherical	401	8933	385	-------	-------
PCM	------	0.372 (solid) 0.151 (liquid)	1004 (solid) 853-886 (liquid)	2100 (solid) 2090 (liquid)	-------	157.8

Table 6.2. Specifications of shell and tube condenser and operating conditions

Parameters	**Values**
Tube outside diameter, d_o, (mm)	22.22
Thickness of the tube, t_w, (mm)	0.7112
Length of the tube, L, (mm)	15000
Number of tubes, N_t	26064
Number of passes, N_p	1
Condenser surface area, A_o, (m^2)	27292
Thermal conductivity of tube, k_w, (W/m. K)	21.85
Steam flow rate, m_s (kg/s)	270.645
Temperature of condensate at hot well outlet, (^oC)	42.6
Condenser pressure, kPa	8.9
Coolant inlet temperature, T_{c1}, (^oC)	29
Hours of operation in year, τ, (hour)	8000
Price of electrical energy, $\phi_{e,}$ ($/kWh)	0.011

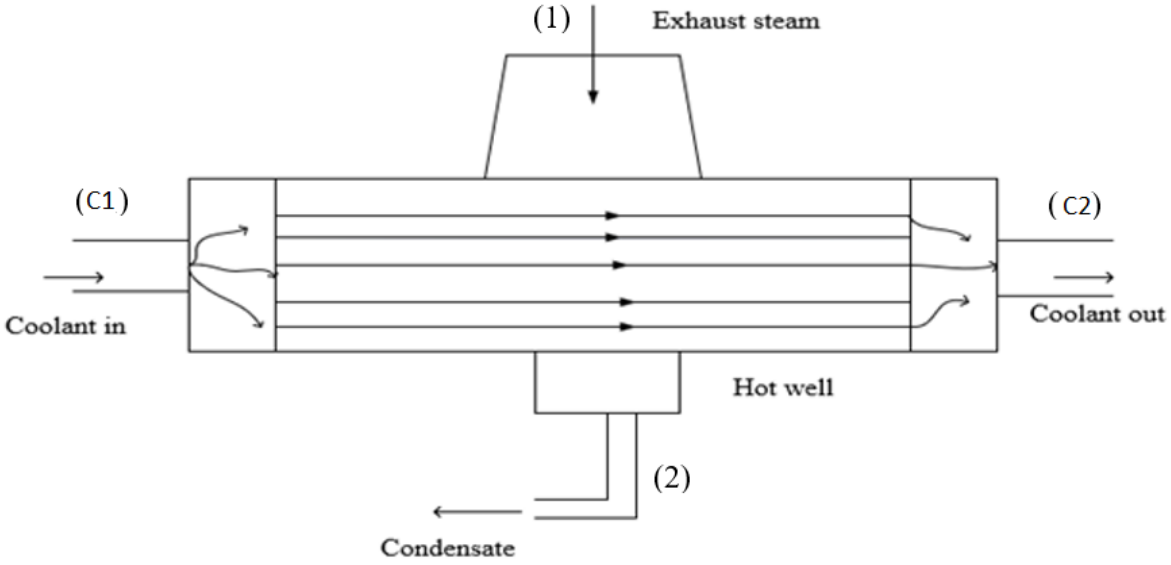

Figure 6.1. Layout of studied shell and tube condenser

6.1.1 Thermophysical properties of hybrid nanofluid

The density of hybrid nanofluid has been calculated by **(Sarkar et al., 2015)**,

$$\rho_{nf} = \phi_{p1}\rho_{p1} + \phi_{p2}\rho_{p2} + (1-\phi)\rho_{bf} \tag{6.1}$$

where ϕ is the overall volume concentration of two different types of nanoparticles (p1 and p2) dispersed in hybrid nanofluid and is calculated as,

$$\phi = \phi_{p1} + \phi_{p2} \tag{6.2}$$

The heat capacity of hybrid nanofluid can be determined as follows **(Sarkar et al., 2015)**:

$$c_{pnf} = \frac{\phi_{p1}\rho_{p1}c_{pp1} + \phi_{p2}\rho_{p2}c_{pp2} + (1-\phi)\rho_{bf}c_{pbf}}{\rho_{nf}} \tag{6.3}$$

Thermal conductivity is the most vital properties, which is responsible for improved heat transfer. **Sahu and Sarkar (2019)** proposed a new model to determine the thermal conductivity and viscosity of the hybrid nanofluid, which have been used in this investigation. The effective thermal conductivity of hybrid nanofluids having different shape nanoparticles can be calculated by using the interpolation method,

$$k_{nf} = \frac{\phi_1 k_{nf1} + \phi_2 k_{nf2}}{\phi} \tag{6.4}$$

Where k_{nf1} and k_{nf2} are the thermal conductivity of mono nanofluid having the same type of nanoparticles with concentration ϕ, which are given by (**Sahu and Sarkar (2019))**,

$$\frac{k_{nf1}}{k_{bf}} = \frac{k_{p1} + 2k_{bf} + 2\phi(k_{p1} - k_{bf})}{k_{p1} + 2k_{bf} - \phi(k_{p1} - k_{bf})} \quad \text{(nanoparticle 1 of spherical shape)} \tag{6.4a}$$

$$\frac{k_{nf2}}{k_{bf}} = \frac{k_{p2} + 2k_{bf} + 2\phi(k_{p2} - k_{bf})}{k_{p2} + 2k_{bf} - \phi(k_{p2} - k_{bf})} \quad \text{(nanoparticle 2 of spherical shape)} \tag{6.4b}$$

$$\frac{k_{nf2}}{k_{bf}} = \frac{k_{p2} + 3.9k_{bf} + 3.9\phi(k_{p2} - k_{bf})}{k_{p2} + 3.9k_{bf} - \phi(k_{p2} - k_{bf})} \quad \text{(nanoparticle 2 of cylindrical shape)} \tag{6.4c}$$

Then, the effective viscosity of hybrid nanofluids having different shape nanoparticles can be calculated by using the interpolation method (**Sahu and Sarkar (2019))**,

$$\mu_{nf} = \frac{(\mu_{nf1}\phi_1 + \mu_{nf2}\phi_2)}{\phi} \tag{6.5}$$

Similarly, the viscosity of nanofluid having different shape nanoparticles is given by,

$$\mu_{nf1} = \mu_{bf}(1 + 2.5\phi + 6.2\phi^2) \quad \text{(nanoparticle 1 of spherical shape)} \tag{6.5a}$$

$$\mu_{nf2} = \mu_{bf}(1 + 2.5\phi + 6.2\phi^2) \quad \text{(nanoparticle 2 of spherical shape)} \tag{6.5b}$$

$$\mu_{nf2} = \mu_{bf}(1 + 13.5\phi + 904.4\phi^2) \quad \text{(nanoparticle 2 of cylindrical shape)} \tag{6.5c}$$

6.1.2 Energetic Modelling

The steam, exhausted from the turbine, is flowing through the shell side of the condenser with the flow rate of m_s. Condenser heat load, q, is given by,

$$q = m_s(h_1 - h_2) \tag{6.6}$$

Where h_1 and h_2 are enthalpies of steam inlet and condensate exit, respectively.

Coolant (proposed hybrid nanofluid) is passing through the condenser's tubes. The mass flow rate of hybrid nanofluid $\dot{m}_c$ is given by,

$$q = m_c c_{pnf} (T_{c2} - T_{c1}) \tag{6.7}$$

Where T_{c1} and T_{c2} are the inlet and outlet temperatures of the coolant, respectively.

In the case of PCM hybrid nanofluid, if melting temperature is in between T_{c1} and T_{c2},

$$q = m_c \left[c_{pnf} (T_{c2} - T_{c1}) + \phi_{PCM} \left(\rho_{PCM} / \rho_{nf} \right) L_{PCM} \right] \tag{6.7a}$$

The coolant mean velocity, u_m, is given by

$$m_c = u_m \rho_{nf} \frac{\pi}{4} d_i^{\,2} N_t \tag{6.8}$$

Where N_t and d_i are the number of tubes and the inside diameter of the tube, respectively.

The tube side Reynolds number is calculated by,

$$\mathrm{Re}_{nf} = \frac{\rho_{nf} u_m d_i}{\mu_{nf}} \tag{6.9}$$

Also, the Prandtl number is given by,

$$\mathrm{Pr}_{nf} = \frac{c_{pnf} \mu_{nf}}{k_{nf}} \tag{6.10}$$

Since the flow is turbulent, **Xuan and Li (2003)** correlation for turbulent flow inside a tube has been used, which is given by,

$$Nu = \frac{\alpha_i d_i}{k_{nf}} = 0.0059 \left(1 + 7.6286 \phi^{0.6886} Pe_{nf}^{\;0.001} \right) \mathrm{Re}_{nf}^{\;0.9238} \mathrm{Pr}_{nf}^{\;0.4} \tag{6.11}$$

Where α_i is the convective heat transfer coefficient and Pe_{nf} is the particle Peclet number, which is given by,

$$Pe_{nf} = \frac{\rho_{nf} c_{pnf} u_m d_p}{k_{nf}} \tag{6.12}$$

Where d_p is the particle diameter.

The overall heat transfer coefficient, U_o, based on tube outside diameter, is given by **(Kakac et al., 2012)**,

$$U_o = \frac{1}{\alpha_o} + R_{ft} \tag{6.13}$$

Where R_{ft} is the sum of all other thermal resistance which is given by,

$$R_{ft} = R_{fo} + \left[\frac{1}{\alpha_i} + R_{fi} \right] \frac{d_o}{d_i} + \frac{t_w d_o}{k_w D_m} \tag{6.14}$$

Where R_{fi} and R_{fo} are the fouling resistances and their values assumed to be as 0.00018 and 0.00009 m^2K/W, respectively. Also, k_w and t_w, are tube wall thermal conductivity and wall thickness, respectively. And D_m is approximated as,

$$D_m = \frac{d_o - d_i}{\ln\left(d_o / d_i\right)} \approx \frac{1}{2}\left(d_o + d_i\right) \tag{6.15}$$

The condensing side heat transfer coefficient, α_o, may be calculated by Nusselt method with Kern correction for condensate inundation,

$$\alpha_o = 0.728 \left[\frac{\rho_l^{\,2} g h_{\lg} k_l^{\,3}}{\mu_l \Delta T_w d_o} \right]^{1/4} \frac{1}{N^{1/6}} \tag{6.16}$$

Where N, the average number of tube rows in a vertical column and ΔT_w is the difference between the saturation temperature and the temperature at the surface of the fouling.

The temperature difference, ΔT_w, is given by,

$$\Delta T_w = \Delta T - R_t q'' \tag{6.16a}$$

Where, ΔT is the local temperature difference between the fluids, R_t is the sum of all other resistances and q'' is the local heat flux, which is given by,

$$q'' = U\Delta T \tag{6.16b}$$

The value ΔT_w has been evaluated by using the iteration method.

The heat transfer rate is given by

$$q = U_o A_o \Delta T_{lm} \tag{6.17}$$

Where A_o surface area which is given by

$$A_o = \pi . d_o . L . N_t \tag{6.18}$$

Where d_o and L are the outside diameter and length of the tube, respectively.

ΔT_{lm} is the logarithmic mean temperature difference, which given by,

$$\Delta T_{lm} = \frac{\left(T_{sat} - T_{c1}\right) - \left(T_{sat} - T_{c2}\right)}{\ln\left(\frac{T_{sat} - T_{c1}}{T_{sat} - T_{c2}}\right)} \tag{6.19}$$

The pressure drop in the tube side can be determined by,

$$\Delta p_t = 4 f \frac{L . N_p}{d_i} \frac{G^2}{2\rho_{nf}} + 4 N_p \frac{\rho_{nf} . u_m^{\ 2}}{2} \tag{6.20}$$

Where Np is number of passes, assumed to be 1. f is the friction factor and G is the mass velocity, given by, respectively **(Kakac et al., 2012)**,

$$f = 0.3108 \,\mathrm{Re}_{nf}^{\ -0.245} \left(1 + \phi\right)^{0.42} \tag{6.21}$$

$$G = \rho_{nf} u_m \tag{6.22}$$

The pumping power is proportional to the pressure drop across the condenser,

$$W_P = \frac{m_c \Delta p_t}{\rho_{nf} \eta_P} \tag{6.23}$$

Where η_p is the efficiency of the pump.

The effectiveness of the shell and tube condenser is the ratio of the temperature difference of the cold fluids to the maximum temperature difference between cold fluid and hot steam, which can be calculated as,

$$\varepsilon = \frac{(T_{c2} - T_{c1})}{(T_{sat} - T_{c1})} \tag{6.24}$$

6.1.3 Exergetic Modelling

The exergy is not conserved due to irreversibilities in the system. Irreversibility is equivalent to the exergy destroyed, which is proportional to the entropy generation. In this study, the exergy loss by hot fluids (steam), Ex_{hot}, is given by,

$$Ex_{hot} = q - m_s T_a (s_{s1} - s_{s2}) \tag{6.25}$$

Where, s_{s1} and s_{s2} are specific entropy of steam at inlet and entropy of condensate at the outlet of condenser, respectively, and T_a is ambient temperature.

And, exergy gain by cold fluid (hybrid nanofluids), Ex_{nf} is given by,

$$Ex_{nf} = q - m_c T_a \left[c_{pnf} \ln\left[\frac{T_{c2}}{T_{c1}}\right] - \frac{\Delta p_t}{\rho_{nf} T_{avg}} \right] \tag{6.26}$$

Where, $T_{avg} = \frac{T_{c1} + T_{c2}}{2}$

Now, irreversibility or exergy destruction is defined as the difference between exergy loss by hot fluids and exergy gain by cold fluids, which is given by,

$$I = Ex_{hot} - Ex_{nf} \tag{6.27}$$

The second law efficiency is defined as the ratio of exergy gain by cold fluid to exergy loss by hot fluid, which is given by,

$$\eta_{II} = \frac{Ex_{nf}}{Ex_{hot}} \tag{6.28}$$

6.1.4 Economic Modelling

The total operating cost (C_{op}) related to pumping work is given by **(Hajabdollahi et al., 2012)**,

$$C_{op} = W_p \tau \varphi_e \tag{6.29}$$

Where τ is hours of operation in a year and φ_e is cost of power ($/kWh).

Saving of operation cost while using hybrid nanofluids is given by,

$$\Delta C_{op} = C_{op,bf} - C_{op,nf} \tag{6.30}$$

Where $C_{op,bf}$ and $C_{op,nf}$ are the operating costs while using base fluid (water, conventional coolant) and hybrid nanofluid as coolant.

The payback period (PBP) determines the duration in which the use of hybrid nanofluids as coolant would be profitable. For the same system (only conventional coolant is assumed to be replaced by hybrid nanofluid), PBP can be defined as the ratio of the cost increase of coolant to the annual saving in operating cost. Neglecting the base fluid (water) cost, the PBP (expressed in years) can be calculated by,

$$PBP = \frac{C_{np}}{\Delta C_{op}} \tag{6.31}$$

Where C_{np} is the total cost of nanoparticles used in considered hybrid nanofluid.

6.1.5 Simulation and validation

The EES program has been developed based on the modeling presented above. For a given geometry, steam-side operating conditions and coolant inlet temperature, required coolant flow rate, coolant exit temperature and heat transfer rate have been iterated by using Eqs. (6.1-6.20) and then various performance parameters such as coolant saving, pumping power reduction, irreversibility, operating cost saving and PBP have been evaluated. To validate the simulation model, a comparison has been made with the experimental results

collected from the power plant. The present study compares the overall heat transfer coefficient and effectiveness with that of the experimental results using water as a coolant, taking the same heat transfer rate, inlet temperature and dimension. It has been found that a deviation of 7.8% for the overall heat transfer coefficient and 9.4 % for effectiveness has been observed, which is justifiable.

6.2. Results and discussion

6.2.1 Energetic performance

The effect of different types of nanoparticles on the energy performance of the shell and tube condenser has been carried out. For the given load (heat transfer rate), the variation of coolant mass flow rate and reduction of mass flow rate with nanoparticles volume concentrations are shown in Figs. 6.2 and 6.3. It can be found that Al_2O_3+PCM hybrid nanofluid needs a lower mass flow rate and Al_2O_3+Ag needs a higher mass flow rate comparatively. With an increase in nanoparticle volume concentration, the convective heat transfer coefficient increases mainly due to the increase in thermal conductivity. Hence, the overall heat transfer coefficient enhances with an increase in nanoparticle volume concentration, as depicted in Fig. 6.4. At 1% volume concentration, Al_2O_3+Ag hybrid nanofluid shows the highest overall heat transfer coefficient enhancement (about 3.2%) followed by Al_2O_3+Cu (about 3.1%), Al_2O_3+TiO_2 (about 2.99%), Al_2O_3+MWCNT (about 2.93%) and Al_2O_3+PCM (about 2.87%) hybrid nanofluids as compared to the base fluid. It can be noted that the requirement of coolant mass flow rate depends on both heat transfer coefficient and heat capacity, which show opposite trends (heat transfer coefficient increases, which is favorable, whereas heat capacity decreases, which is unfavorable) with volume fraction. Hence, with the increase in volume concentration, the requirement of coolant mass flow rate decreases due to the predomination of heat transfer coefficient and then increases due to the predomination of heat capacity. The results reveal that the maximum reduction of

mass flow rate for Al_2O_3+PCM hybrid nanofluid is 4.1%, followed by Al_2O_3+MWCNT (3.6%), Al_2O_3+TiO_2 (2.9%), Al_2O_3+Cu (1.5%) and Al_2O_3+Ag (1.3%) as compared to the base fluid. Al_2O_3+PCM has lower thermal conductivity but is most favorable due to both latent heat and heat capacity than others.

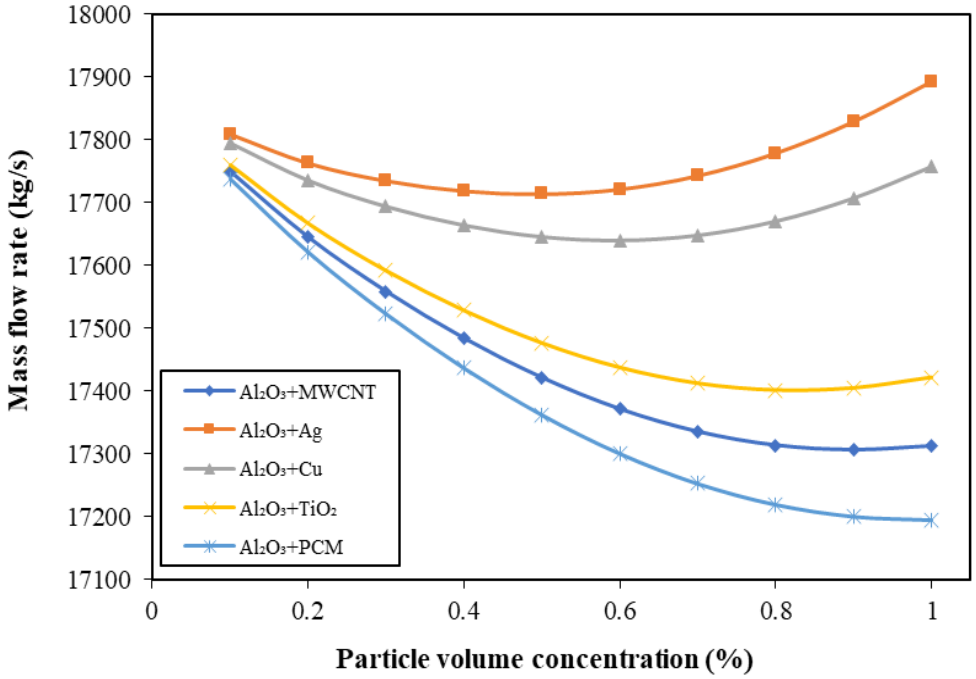

Figure 6.2. Variation of coolant mass flow rate with nanoparticle volume concentration

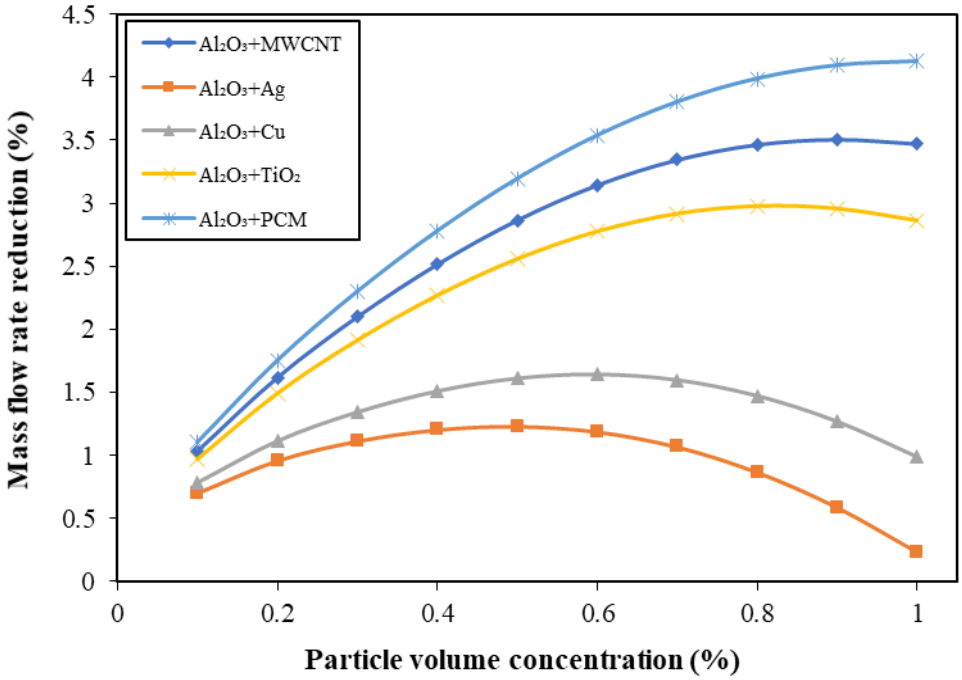

Figure 6.3. Variation of mass flow rate reduction (%) with volume concentration

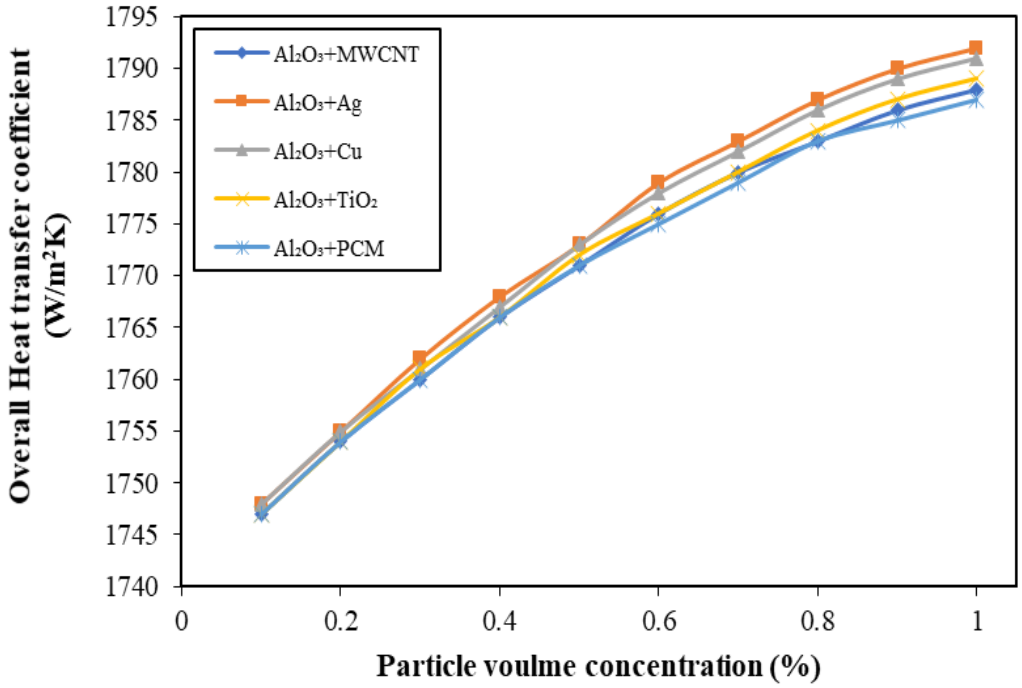

Figure 6.4. Variation of overall heat transfer coefficient with volume concentration

Fig. 6.5 shows the variation of the effectiveness of shell and tube condenser with nanoparticle volume concentration. As shown, the effectiveness of the shell and tube condenser enhances with the addition of nanoparticles due to an increase in the heat transfer coefficient. At 1% volume concentration, Al_2O_3+Ag hybrid nanofluid shows the highest effectiveness enhancement of 6.8%, followed by Al_2O_3+Cu (6.6%), Al_2O_3+TiO_2 (6.4%) and Al_2O_3+MWCNT (6.3%) and Al_2O_3+PCM (6.17%) as compared to the base fluid. As shown in Fig. 6.6, the pressure drop decreases then increases with an increase in nanoparticle volume concentration due to the similar trend of mass flow rate. The results imply that Al_2O_3+PCM hybrid nanofluid shows the maximum reduction in pressure drop among all other hybrid nanofluids. The maximum reduction of the pressure drop of Al_2O_3+PCM hybrid nanofluid is 6.41%, followed by Al_2O_3+MWCNT (6.2%), Al_2O_3+TiO_2 (5.7%), Al_2O_3+Cu (4.5%) and Al_2O_3+Ag (4.0%) at optimum volume concentration as compared to the base fluid. Due to the combined effects of pressure drop (decreases and then increases), mass flow

rate (decreases and then increases) and density (increases) with nanoparticle volume concentrations, the pump work requirement decreases (Fig. 6.7). The result indicates that Al_2O_3+PCM requires 11.36% less pump work at 1% volume concentration followed by Al_2O_3+MWCNT (11.2% less), Al_2O_3+TiO_2 (10.9% less), Al_2O_3+Cu (10.2% less) and Al_2O_3+Ag (9.6%) as compared to the base fluid.

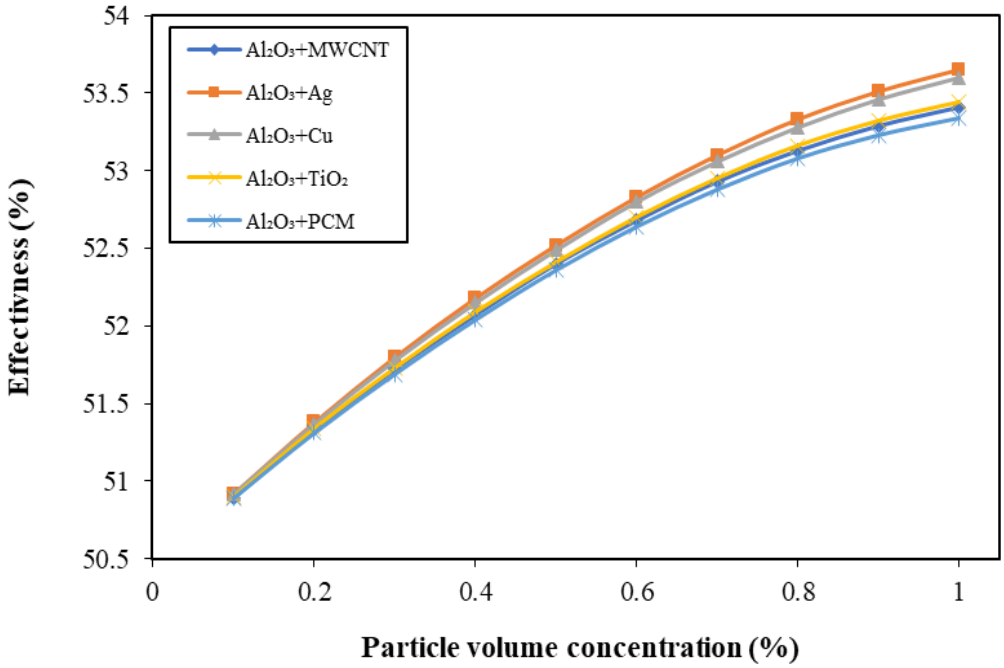

Figure 6.5. Variation of condenser effectiveness with nanoparticle volume concentration

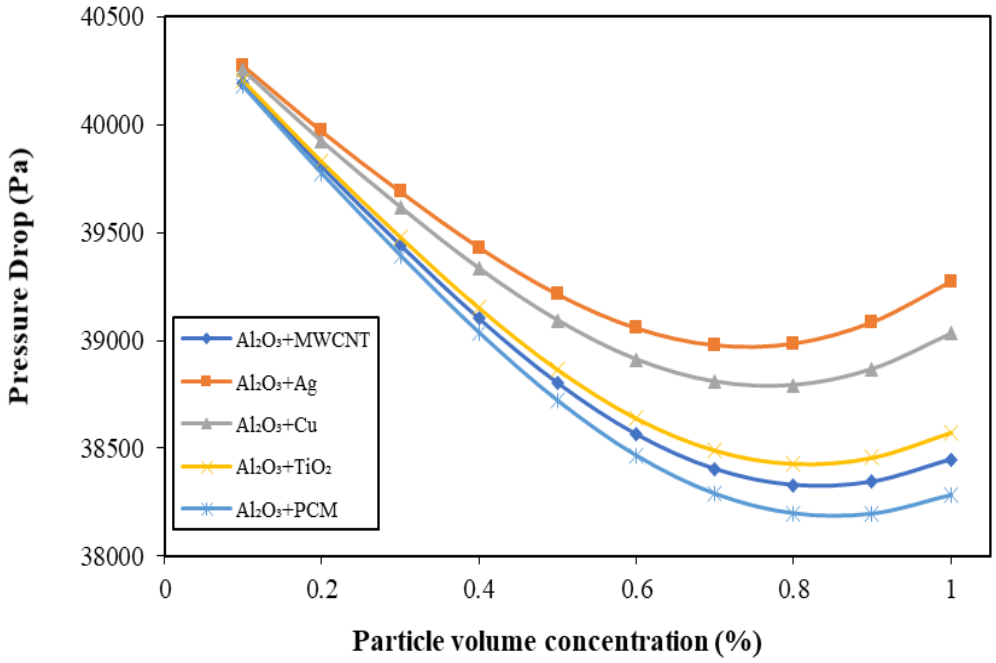

Figure 6.6. Variation of coolant pressure drop with nanoparticle volume concentration

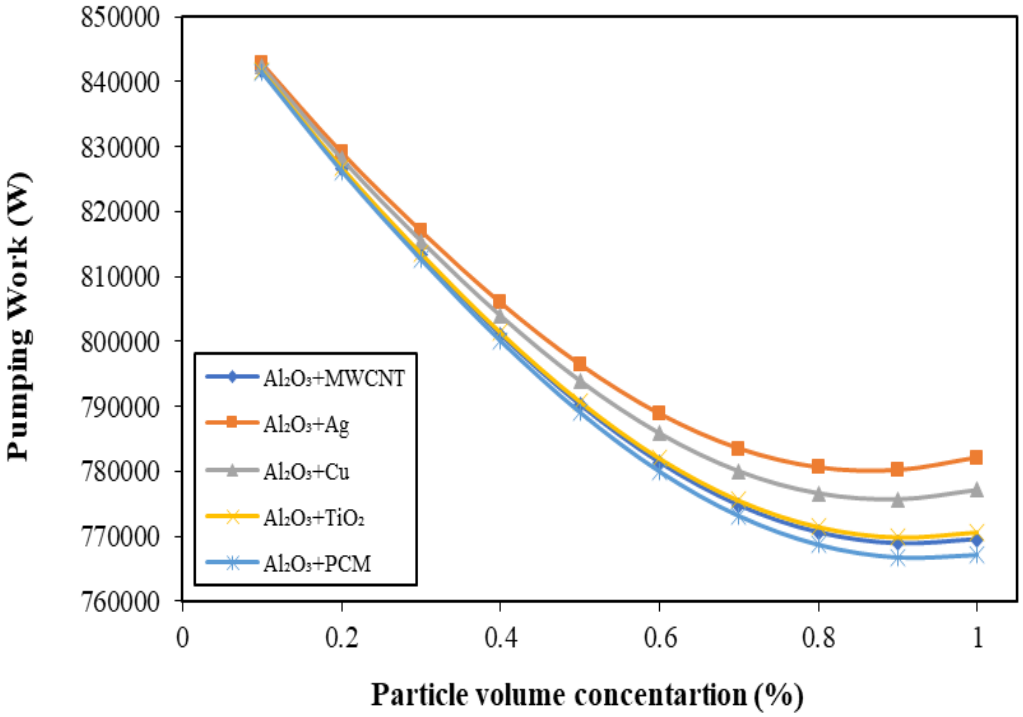

Figure 6.7. Variation of pumping power with nanoparticle volume concentration

6.2.2 Exergetic performance

The variation of irreversibility with volume concentration is shown in Fig. 6.8. The result reveals that irreversibility decreases with the addition of nanoparticles due to an increase in heat transfer coefficient and hence a decrease in temperature difference. At 1% volume concentration, Al_2O_3+Ag hybrid nanofluid shows minimum irreversibility, followed by Al_2O_3+Cu, Al_2O_3+TiO_2, Al_2O_3+MWCNT and Al_2O_3+PCM. In terms of percentage reduction, Al_2O_3+Ag shows a maximum of 2.08% and Al_2O_3+PCM shows a minimum of 1.79% reduction at 1% volume concentration. Another reason is that the variation of irreversibility is a function of entropy generation, which depends upon heat capacity rate, inlet and outlet temperature of the coolant. Since the mass flow rate and specific heat decreases, the irreversibility decreases with an increase in volume concentration. With an increase in volume concentration, the second law efficiency shows increasing trends, as

shown in Fig. 6.9. Among all hybrid nanofluids, Al_2O_3+Ag shows maximum (29.97%) and Al_2O_3+PCM shows minimum (29.77%) second law efficiency at 1% volume concentration.

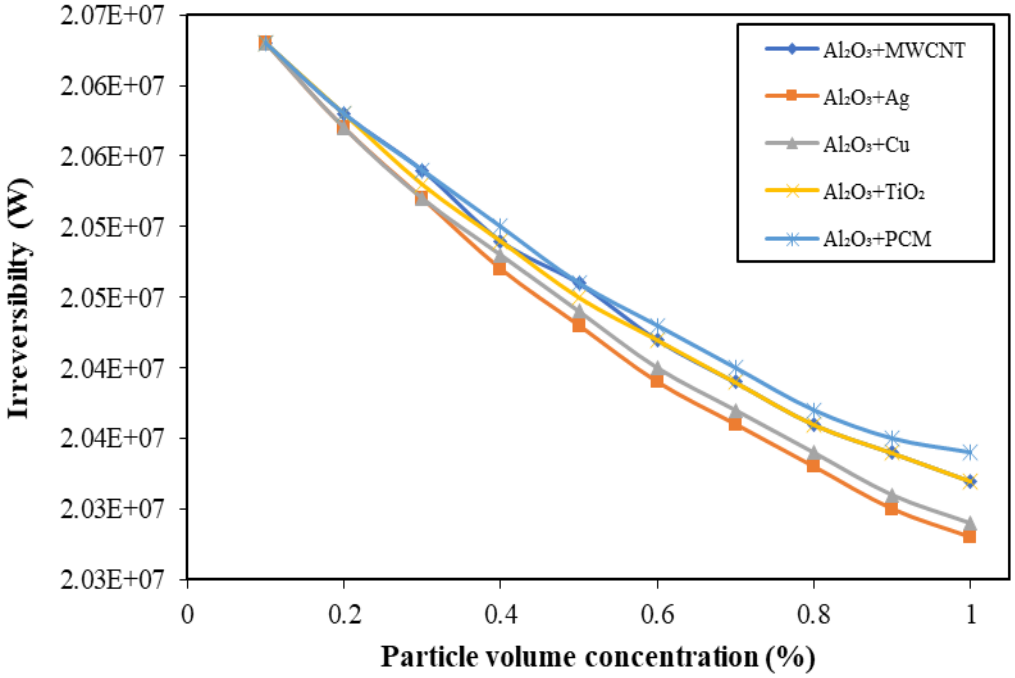

Figure 6.8. Variation of irreversibility with nanoparticle volume concentration

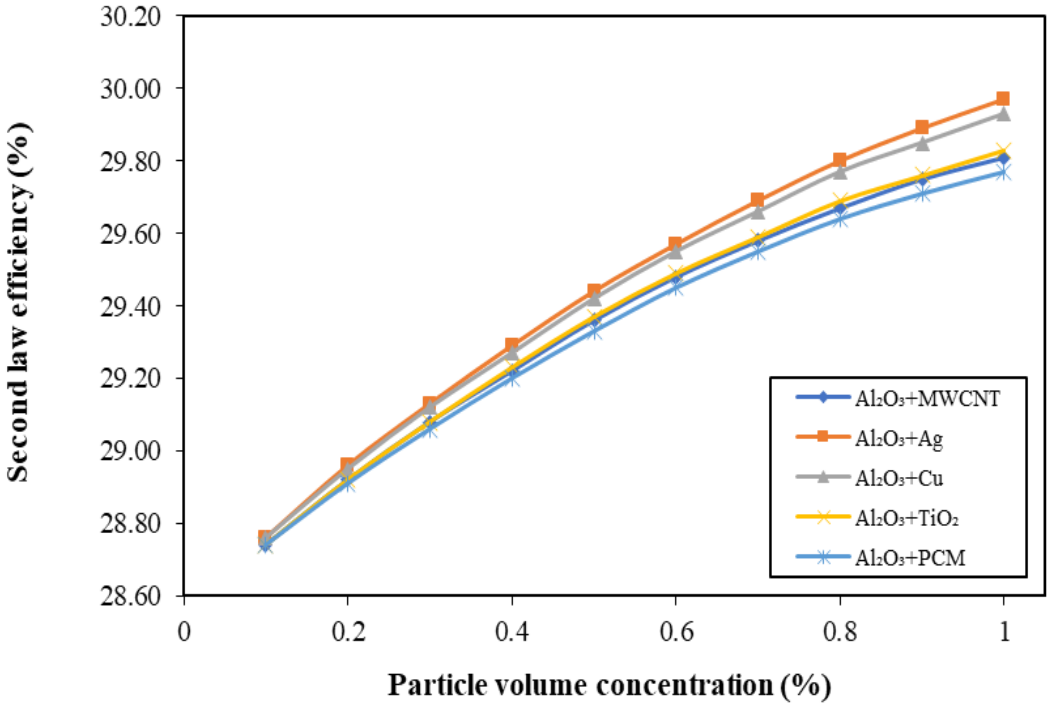

Figure 6.9. Variation of second law efficiency with nanoparticle volume concentration

6.2.3 Economic performance

The variation of operating cost with volume concentration is shown in Fig. 6.10. The results showed that the operating cost decreased with the addition of nanoparticles. Since the pumping power decreases with nanoparticle volume concentration, the operating cost decreases with the addition of the nanoparticles. At 1% volume concentration, the operating cost using Al_2O_3+PCM hybrid nanofluid is minimum and using Al_2O_3+Ag hybrid nanofluid is maximum. In terms of saving operating cost, using Al_2O_3+PCM hybrid nanofluid shows a maximum of 11.4% and using Al_2O_3+Ag hybrid nanofluid shows a minimum of 9.62% at 1% volume concentration, compared to the base fluid, as shown in Fig. 6.11. The variation of the payback period (PBP) with volume concentration is shown in Fig. 6.12. The results reveal that at 1% volume concentration, Al_2O_3+Ag shows maximum PBP about 247 years, followed by Al_2O_3+Cu (about 90 years), Al_2O_3+MWCNT (about 63 years), Al_2O_3+TiO_2 (9.8 years) and Al_2O_3+PCM (about 6.24 years). The reason is that the cost of nanofluids increases with an increase in volume concentration as the PBP is the ratio of the cost of nanofluids to saving in the operating cost. It has been observed that Al_2O_3+Ag gives the maximum PBP, which is far away from the depletion life of the equipment. This is due to the high cost and requirement of the Ag nanoparticles (higher density needs higher mass). Assuming 10 years of equipment's life, the results show that only Al_2O_3+TiO_2 and Al_2O_3+PCM hybrid nanofluid give PBP below the equipment's life because of the cheap cost of the nanoparticles. Hence, hybrid nanofluid is not a suitable candidate for practical use in the present cost scenario due to very high PBP. However, the PBP can be significantly reduced by increasing hybrid nanofluid operational stability (use of the same nanofluids for a long time), decreasing to nanofluids total volume used, or decreasing nanoparticle unit price of nanoparticles. For example, with a 20% reduction of nanoparticle amount or unit price of nanoparticles, the PBP

for Al_2O_3+Ag hybrid nanofluid reduces from 194.2 to 155.4 years and from 51.5 to 41.2 years for Al_2O_3+MWCNT, which are still high. Hence, a significant reduction of unit nanoparticle price is required before practical implementation in a power plant.

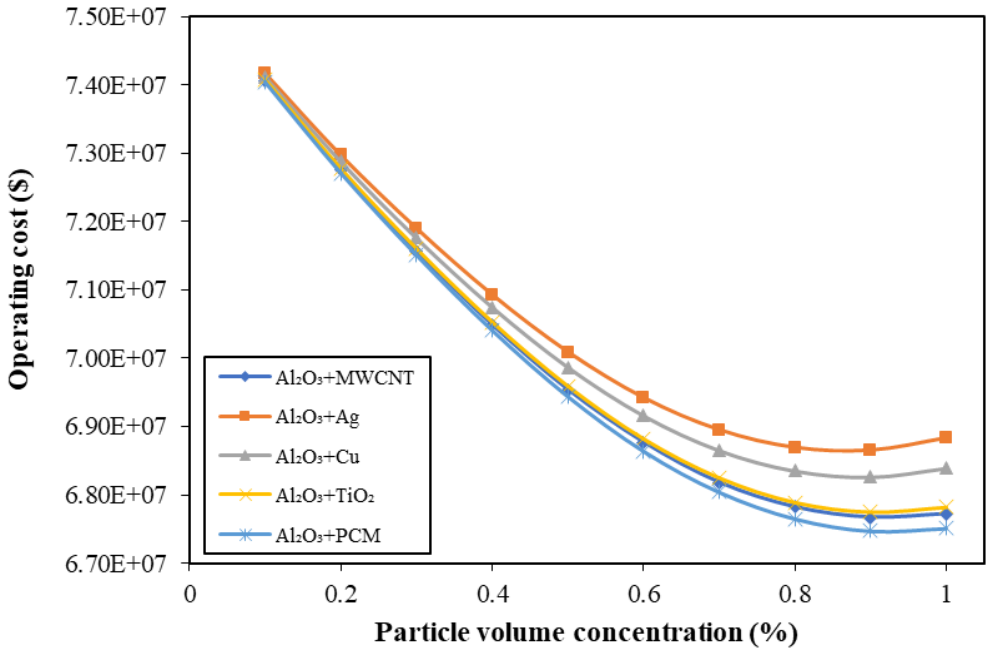

Figure 6.10. Variation of operational cost condenser with nanoparticle volume concentration

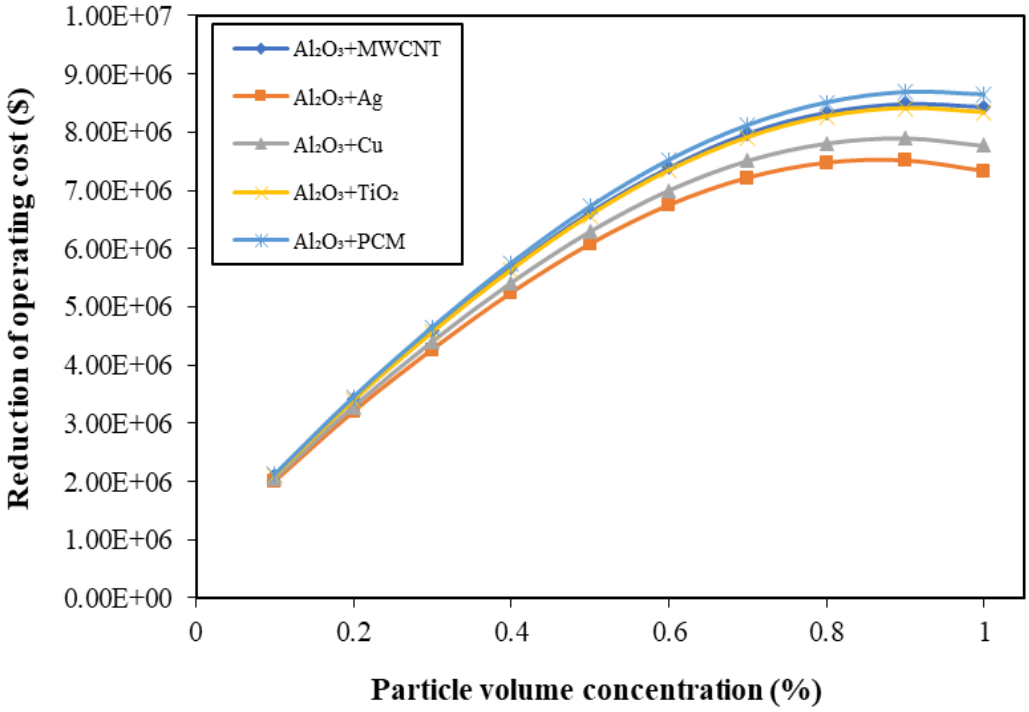

Figure 6.11. Variation of operational cost reduction with nanoparticle volume concentration

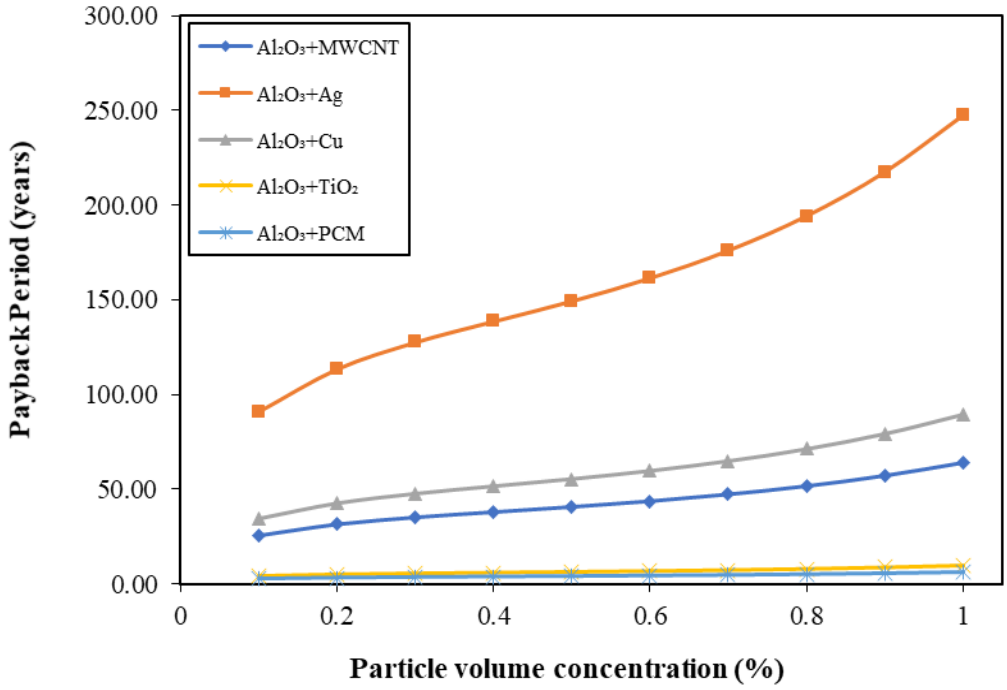

Figure 6.12. Variation of payback period with nanoparticle volume concentration

6.3. Highlights

The energy, exergy and economic performances of industrial shell and tube condenser using different water-based hybrid nanofluids such as Al_2O_3+MWCNT, Al_2O_3+Ag, Al_2O_3+Cu, Al_2O_3+TiO_2 and Al_2O_3+PCM under turbulent flow have been numerically investigated. Based on the results and discussion, the following conclusions can be made:

- The requirement of coolant mass flow rate can be reduced by using hybrid nanofluid (Al_2O_3+PCM yields the highest reduction of 4.1%, followed by Al_2O_3+MWCNT, Al_2O_3+TiO_2, Al_2O_3+Cu and Al_2O_3+Ag as compared to base fluid). The effectiveness is also enhanced by using hybrid nanofluids.
- Coolant side pressure drop, as well as pumping power, can be reduced by using hybrid nanofluids. Pumping power reduction is maximum for Al_2O_3+PCM (11.36%) and minimum for Al_2O_3+Ag (9.6%).

- The irreversibility decreases and second law efficiency increases with the addition of nanoparticles. Al_2O_3+Ag shows maximum second law efficiency (29.97%) and Al_2O_3+MWCNT shows minimum (29.81%) at 1% volume concentration.
- The operating cost can be reduced with the addition of the nanoparticles. In term of saving of operating cost, Al_2O_3+PCM hybrid nanofluid shows a maximum of 15.69% and Al_2O_3+Ag hybrid nanofluid shows a minimum of 9.62% at 1% volume concentration, compared to the base fluid.
- The payback period is considerably higher for the use of hybrid nanofluid (Al_2O_3+Ag shows a maximum of 247 years and Al_2O_3+PCM shows a minimum of 6.24 years). PBP can be reduced by reducing nanoparticle cost and increasing nanofluid stability.

The engineering applications of the modeling techniques would improve the usage of nanofluids; however, their application has been much relatively insignificant in the existing industrial condensers. This simulation modeling is mainly used in the various forms of heat exchangers such as solar collectors, microchannels, car radiators, cooling electronic devices, etc. Moreover, a new model which determine the physical properties of the hybrid nanofluid with different nanoparticles shape can be used for investigating other engineering applications.